DOI: 10.15199/17.2023.12.1

Influence of hydrogen blended gas transmission under transient flow on L485ME steel grade fracture toughness

Wpływ mieszaniny gazu z wodorem w stanie nieustalonego przepływu na odporność na pękanie stali L485ME

Ferdinand Uilhoorn and Maciej Witek*

Keywords: *hydrogen embrittlement; fracture toughness; hydrogen induced cracking; transient flow model; L485ME steel grade*

Abstract
In the present study, the L485ME low-alloy steel grade, widely used in the last few decades in the natural gas transmission pipelines, subjected to hydrogen was investigated with respect to material degradation. A fracture toughness parameter such as the calculated conditional stress intensity factor was compared to the threshold stress intensity factor for the plane strain hydrogen-assisted cracking derived from the experimental data. Based on macroscopic and microscopic evaluation and measurements, the hydrogen-assisted crack size propagation in steel specimens was compared to the subcritical crack growth. The hydrogen content in the tube wall for the base metal and heat-affected zone was estimated, whereas the pressure and temperature conditions in the pipeline were calculated from a non-isothermal transient gas flow model. The results were used to estimate the fracture toughness of the pipe wall material exposed to the hydrogen-blended natural gas.

Słowa kluczowe: *kruchość wodorowa; odporność na pękanie; pękanie wywołane wodorem; model nieustalonego przepływu; gatunek stali L485ME*

Streszczenie
W niniejszej pracy została przebadana, pod kątem degradacji materiału na skutek działania wodoru, stal niskostopowa gatunku L485ME, szeroko stosowana w ostatnich dziesięcioleciach do budowy rurociągów przesyłowych gazu ziemnego. Parametr odporności na kruche pękanie, taki jak obliczeniowy warunkowy współczynnik intensywności naprężeń, porównano z granicznym współczynnikiem intensywności naprężeń dla wydłużenia płaskiego, który wyznaczono z danych doświadczalnych dla pękania wywołanego wodorem. Na podstawie oceny oraz pomiarów makroskopowych i mikroskopowych, porównano wspomaganą wodorem propagację wielkości podkrytycznego wzrostu pęknięć w próbkach stalowych. Oszacowana została zawartość wodoru w ściance rury dla metalu podstawowego oraz strefy wpływu ciepła. W oparciu o nieizotermiczny model przepływu gazu w stanie nieustalonym, obliczono warunki ciśnienia i temperatury w rurociągu. Uzyskane wyniki wykorzystano do oszacowania odporności na pękanie materiału ścianki rury poddanego działaniu gazu ziemnego z dodatkiem wodoru.

1. Introduction

The most important issue for injection of hydrogen, generated from renewable energy sources, to the gas transmission network is whether pipelines constructed from thermomechanically rolled steels, widely used in the last few decades, are suitable for hydrogen (H_2) blended natural gas (C_xH_y/H_2). It should be considered what percentage of C_xH_y/H_2 mixtures in gas transmission pipelines with pressures up to 10 MPa is allowable from the tube steel grade application point of view. The overall literature consensus is that the interaction of several mechanisms is responsible for the low-alloy steel degradation caused by hydrogen [9]. In respect of structural integrity of tubes, transmission of C_xH_y/H_2 blends in a gaseous form using steel pipelines, introduces a possible decrease in mechanical properties such as ductility of steel (elongation to failure), fracture toughness and material fatigue performance.

Hydrogen can enter the pipe wall material from both internal and external sources. The internal source is related to steel processing, i.e., welding or steelmaking manufacturing. Along with hydrogen dissociation out of the moisture from atmosphere surrounding montage welding in field, this phenomenon can cause high susceptibility to embrittlement of the tube joints [22]. During construction of steel pipelines suitable for C_xH_y/H_2 mixtures transportation, it is generally accepted that the hardness of the material connecting the pipe joints should be limited to approximately 235 HV10 in order to reduce a risk of hydrogen cracking in the weld area and the heat-affected zone. The above requirement, related to the hardness, causes a necessity of appropriate heat treatment during montage welding in field performed during the pipeline construction. However, the present investigation does not consider neither welding quality records nor procedures of preparation of joint connecting the pipelines constructed from L485M steel grade [2] (API notation X70M [1]) and used for blended natural gas transportation. The only weld metals considered in the present study are seams on the tube body.

However, only an atomic form of H absorption into the steel may occur from external sources, such as electrolytic process from

*) **Ferdinand Uilhoorn and Maciej Witek** – Warsaw University of Technology, Gas Engineering Group, Nowowiejska 20, 00-653 Warsaw, Poland. e-mail: ferdinand.uilhoorn@pw.edu.pl and maciej.witek@pw.edu.pl.

cathodic protection or H_2 trapping in a gaseous form. Presence of pressurized H_2 in gas pipelines, originally designed for natural gas, generates an additional external source for diffusion and solubility of hydrogen. The current research investigates 30 % and 50 % hydrogen contents in the transported gas mixture using L485ME steel grade tubes [1, 2], which are commonly used worldwide for pipeline projects originally designed for natural gas.

The role of microstructure is one of the most important factors to be considered in terms of susceptibility of steel degradation caused by hydrogen. For a welded pipes, three different microstructural zones are required to be considered in terms of HE: the base metal (BM), weld metal on the tube body (WM) and the heat-affected zone (HAZ). In general, microstructures found in the base material of low carbon steels are: ferrite (polygonal, acicular and bainitic), pearlite, bainite (lower an upper), austenite and martensite. The ferritic microstructure in pipeline steels is modified in the welded areas. For this reason, additional microstructures are present in weld metals on the pipe body and in heat-affected zones [20, 21].

Microstructural aspects are strongly dependent on the manufacturing process of the tubes, which finally affects both diffusion and trapping of hydrogen. H atoms occupy interstitial sites in the lattice of the base material or locate at microstructural features. Potential locations for hydrogen trapping include dislocations, grain boundaries, second-phase particles, voids and interstitial solute atoms, and depends on the steel microstructure. Hydrogen-induced cracking (HIC) in pipeline steels is mainly controlled by local hydrogen concentration, depending on where hydrogen is trapped. As H atoms strongly interact with hydrostatic stress fields, they are easily trapped in the dislocations generated prior to deformation, thus hindering hydrogen diffusion. The main hydrogen trapping sites in the ferritic-pearlitic microstructure are ferrite-pearlite interfaces, elongated manganese sulphide MnS inclusions, and the ferrite-cementite interfaces in lamellar pearlite grains. In steels with ferritic-pearlitic microstructure, the dominant diffusion paths are ferrite and ferrite in pearlite for the steady-state hydrogen-diffusion case. While for unsteady-state hydrogen diffusion, analysed in the present paper, the ferrite-cementite interface in pearlite, as a typical hydrogen trap location during the steady-state diffusion, loses its trapping effects and become an active and preferential diffusion path. Paper [27] investigates an influence of hydrogen on the candidate fracture toughness (K_Q) of low carbon steel immersed in acidic hydrogen environments pH 2.5, pH 5.0 for one year. Based on the test results, models for the degradation of K_Q of steel were developed in accordance with the proposed hydrogen-enhanced localized plasticity (HELP) and hydrogen-enhanced decohesion (HEDE) model (HELP + HEDE model) of hydrogen embrittlement. Furthermore, fractography of the specimens was performed to observe the synergistic action of HELP and HEDE mechanisms, and their subsequent effects on the microstructure and fracture resistance of steel.

Grain refinement is also found to have contradictory effects on the hydrogen diffusivity. Firstly, as the grain size decreases, the hydrogen diffusion increases due to a larger grain boundary area. On the contrary, there can also occur an increased hydrogen trapping effect, due to a larger grain boundary network. A microstructure consisting of several fine-grained grains also presents a much higher density of triple junctions, which are the most favorable traps for H_2 atoms, due to lowest trapping energy [30]. In [29], the grain size effect on hydrogen diffusivity of L485M steel grade is studied. As a result of the twofold effects, a diffusion coefficient is maximized for a specific grain size, referred to as a grain boundary cross effect [16]. It has been found for pipeline steel that the maximum diffusion occurs at intermediate grain sizes, and slower diffusion rates occurs for fine and considerably coarse microstructures.

The effect of hydrogen on strength properties of HAZ has been found to be higher than in the base metal and correlates to a higher hydrogen absorption by the microstructure which was mainly acicular ferrite. The amount of diffusive hydrogen is also affected by a microstructure with a different grain size and percentage of the hard phase of the base metal under different rolling conditions. The major microstructure in the heat-affected zones is acicular ferrite. This microstructure contains several features tending to trap hydrogen, such as high dislocation density and fine grains. Latifi [19] studied the effect of a microstructure on hydrogen diffusivity by testing both the base and weld metal of X65 pipeline steel. The results of his research showed that the ferritic matrix and the pearlite/bainite islands in the base metal indicated the lowest diffusion while the most diffusive hydrogen was found in the acicular ferritic microstructure in the weld metal. Fracture surface analysis of both investigated in [14], steel grades, S690QL structural steel and X80 pipeline steel, indicated a transition from a ductile fracture mode to a cleavage dominated fracture mode, due to in-situ hydrogen charging. Hydrogen-induced surface cracks, originated during the plastic deformation regime, lead to lower overall ductility of the investigated materials.

Non-alloy steel encompasses all grades in which the content of specific elements is less than certain limit values. However, in low alloy steels, there are, besides carbon, other alloying additives, present in small amounts. The proportion of a given element is not supposed to exceed 1% by weight [28]. In order to obtain a combination of mechanical properties required for certain steel grades, a precise selection of alloying elements is necessary. However, some alloying components have an adverse influence on the embrittlement susceptibility of pipeline steels through introducing microstructural features that ultimately affect both diffusion and solubility of hydrogen. This effect is highly dependent on the manufacturing process as well as on heat treatment resulting in different microstructures of the base material [13]. From the perspective of transportation of C_xH_y/H_2 mixtures, the content of the following micro additives is crucial to reduce the risk of hydrogen-induced cracking on inclusions:

Sulphur (S) – the maximum content for welded as well as seamless pipes is 0.015 % by weight, according to Table A.1 of EN-ISO 3183; however, for hydrogen applications, the content of S should be reduced to 0.010 % by weight.

Phosphorus (P) – the maximum content for welded as well as seamless tubes is 0.025 % by weight, according to Table A.1 of EN-ISO 3183; however, for C_xH_y/H_2 blends applications the content of P should be reduced to 0.015 % by weight.

Few publications analyse the calculations and experiments to compare a fracture toughness parameter, namely, a computed conditional stress intensity factor, and a threshold stress intensity factor for plane strain environmentally-assisted cracking. Hydrogen-assisted crack size propagation in steel specimens is compared in the current study to the subcritical crack growth obtained from constant displacement method measurements and a macroscopic/microscopic evaluation. To the authors' best knowledge no one before has applied Sievert's law together with a non-isothermal transient gas flow model for a calculation of the hydrogen content in the tube wall base material and the heat-affected zone. The above application is the novelty of the current research.

2. Characteristics of thermomechanically rolled tubes

In the last few decades, the worldwide most commonly used steel grade for construction of gas transmission networks has been thermomechanically rolled steel according EN-ISO 3183 [2], which is equivalent to the X70M notation of API [1]. The examples of gas pipeline sections in Europe, constructed using this steel grade, are:

- Val de Saône Voisines (Haute-Marne région) – Etrez (Ain région) in France, commissioned in 2016, DN 1200, maximum operating pressure (MOP) 6.8 MPa, L = 188 km;
- Ellund (Germany) – Egtved (Denmark) in 2012, DN 750, MOP 8.4 MPa, L = 95 km;
- Yamal pipeline on Polish territory, commissioned in 1999, DN 1400, MOP 8.4 MPa with a length of L = 685 km;
- Polish – Slovak Gas Interconnector, commissioned in 2022, DN 1000, MOP 8.4 MPa, L = 103 km;
- Gas Interconnection Poland – Lithuania (GIPL), commissioned in 2022, DN 700, MOP 8.4 MPa, with a length of L = 355 km on Polish territory.

Sheets and strips used to produce line pipes for high-pressure gas and oil pipelines are manufactured as longitudinally submerged arc-welded tubes (SAWL) up to 1422 mm (56 in) or helically submerged arc-welded pipes (SAWH) up to 2520 mm (100 in). Seamless pipes (SMLS) for oil and gas applications are produced worldwide only up to a nominal diameter of DN 600. According to [2], tubes are classified as normalized or normalizing rolling (N), thermomechanically rolled (M), quenching and tempering (Q) delivery conditions. The thermomechanically rolled pipes are manufactured as welded tubes only. Annex A for [2] shall be applied for PSL2 pipes when the order of tubes is dedicated for onshore natural gas transportation pipelines in Europe.

The longitudinal joint is manufactured by welding on both sides and the calibration of the pipe is usually carried out with expanders. Helically-welded tubes are produced from steel strips coiled in a spiral, then welded along the coiling edge and cut to the correct final size. Their advantages include a possibility of manufacturing a pipe with a longer unit length, compared to a longitudinally welded pipe, while maintaining the accuracy of dimensions, i.e., non-roundness (ovality) and a diameter, satisfying the requirements of EN-ISO 3183 without a need for calibration. Less favourable features of SAWH pipes are a greater length of the welded seams, produced with the rolling mill, compared to longitudinally welded SAWL pipes, and the resulting risk of a potentially greater number of imperfections of weld joints. Nevertheless, helical welded tubes may have longer unit joints, which, in turn, results in a smaller number of girth welds performed during the pipeline construction.

A controlled process of rolling and heat treatment of high-strength plates and strips with appropriate properties is applied in the case of X70M as thermomechanical-rolled, quenching and tempering. The steels should be fully quenched and manufactured with a technology suitable for fine grain steel. L485ME steel grade, so called a high-strength steel grade, is the first in series [28, 8] and its base material, excluding the weld area and the heat-affected zone, has a ferritic-mixed pearlitic-banitic microstructure. Absence of martensite microstructure can be assumed in a typical base material of X70 steel grade [15]. Martensite microstructure is commonly recognized as one of most susceptible for HE and can be present in HAZ.

3. Sustainability of hydrogen environmental cracking

3.1. Fracture control qualification test of pipeline steel

ASME B31.12 Standard [4] delivers requirements for pipelines with H_2 content from 10 % up to 100 % in a gas mixture and provides a qualification procedure of a steel fracture toughness evaluation for Option A prescriptive design method for a design factor up to 0.50. ASME B31.12 Code delivers a qualification procedure for tube material fracture control for Option B in a performance-based design method for a pipeline design factor up to 0.72. Fracture toughness testing is utilized to determine a threshold stress intensity factor of the materials in compliance with the requirements of the ASME code B31.12 Option B and referenced standards.

A fracture toughness criterion or other method shall be specified to control fracture propagation when a pipeline suitable for transportation of C_xH_y/H_2 blends is designed to operate at a hoop stress over 40% of the specified minimum yield strength. When a fracture toughness criterion is applied, control shall be achieved by ensuring that the tube material presents adequate ductility. The tube material tensile requirements shall be specified on the purchasing specification and shall comply with the chemical and tensile requirements of API 5L [1, 2]. In this paper, Option B was applied with the following requirements. The pipe and weld material shall be qualified for adequate resistance to fracture in H_2 gas at or above the design pressure and at ambient temperature using the applicable rules provided in Article KD-10 of ASME BPV Code Section VIII, Division 3 [5].

The purpose of this test is to qualify the material of the structure by testing three heats of the steels. The threshold stress intensity factor values (KIH) shall be obtained from the thickest section from each heat of the material and a type of the applied heat treatment. The test specimens shall be placed in the final heat-treated condition to be used in pipe manufacturing. A set of three specimens shall be tested from each of the following locations: BM, WM, and HAZ of joints, welded with the same qualified welding procedure specification as intended for the piping manufacturing. A change in the welding procedure requires retesting the welded joints in the scope of WM and HAZ. The test specimens shall be oriented in the transverse longitudinal (TL) axis of forcing direction. If TL specimens cannot be obtained from the weld metal and the heat-affected zone, then longitudinal transverse (LT) specimens may be used. The values of KIH shall be obtained with the use of the test method described in KD-1040 of ASME BPV Code Section VIII, Division 3 [5]. The lowest measured value of KIH shall be used in the pipeline design analysis.

Additional requirements for the pipe material are as follows: (i) phosphorus content of the pipe material shall not exceed 0.015 % by weight; (ii) the tube material shall be manufactured with a practical control of inclusions; (iii) minimum specified yield strength shall not exceed 555 MPa, maximum ultimate tensile strength of the weld metal shall not exceed 760 MPa and the pipe material shall meet all applicable requirements of API PSL2 [2, 1]; (iiii) brittle and ductile criteria specified in ASME B31.12 [4] shall be met.

3.2. Experiments for hydrogen cracking of X70M steel grade

In the case of 22.2 mm wall thickness pipes used for experiments in the present study both a hardness criterion set as less than 235 HV10 as well as percentage of selected micro additives

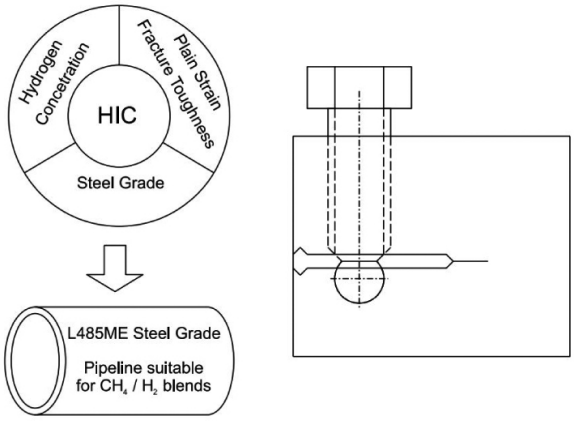

Fig. 1. Graphical representation of the research concept and a sectional view of bolt-load specimen for constant displacement method

Rys. 1. Graficzne przedstawienie koncepcji badań oraz przekrój próbki obciążonej przy pomocy śruby w metodzie stałego przemieszczenia

determined as S ≤ 0.010 %, P ≤ 0.0156 % are met. The steps applied for an experimental evaluation of fracture toughness and a crack size extension are defined according to KD-1041 [5]:

a. The modified bolt-load specimen configuration, as presented in Fig. 1, was utilized in accordance with ASTM E1681-03 international standard [3]. The base metal, the weld metal centre line and HAZ testing locations were used as samples. Thirty L485ME steel grade specimens from BM (12 specimens), WM (9), HAZ (9), were prepared from a 22.2 mm SAWH pipe for fatigue pre-cracking testing, at ambient temperature, in general compliance with ASTM E1681-03 code.
b. A machined notch was further extended through fatigue pre--cracking in ambient temperature conditions. Fatigue pre-cracking testing was performed using Instron Fatigue Propagation Program – Version 8.1 Build 4 following the test control parameters: range – 33 MPa $m^{0.5}$, stress ratio – 0.100, points/cycle – 200, waveform sine frequency – 25 Hz.
c. Specimen bolt-loading (crack opening) was performed in an inert atmosphere (pure N_2), in which oxygen and moisture were stored, and nonstop monitored, below 5 and 50 ppm, as required by the ASME code [4].
d. According to the requirements of ASTM E1681 standard [3], the original precrack size (a0) was measured after fracture at five locations [10].
e. The applied displacement (V_m) was measured with the use of a CMOD-type electronic extensometer. Based on ASTM E1681 §9.1.3 equation [3], the applied displacement was calculated for all specimens in order to exceed the minimum required value of the applied stress intensity factor K_{IA} = 110 MPa $m^{0.5}$, with a typical target of K_{IA} = 125 MPa $m^{0.5}$. According to the provisions of standard ASME BPVC Sec. VIII, Division 3, KD-1041 [5], minimum stress intensity factor $K_{IH,min}$ is equal to 50% of K_{IA}, if the test was applied using the constant displacement method.
f. Having completed the loading of specimens, they were placed in the autoclave which was closed tightly.
g. Next, before being charged with high purity H_2 (grade 6.0), the autoclave was filled with high purity N_2 (grade 6.0) and the pressure was elevated to test value. The working pressure for the experiment was set at a minimum of 8 MPa for a duration of 1000 h.
h. In order to highlight any potential crack propagation, the specimens were heated in the furnace at 3000 °C for 1 h and subsequently broken in liquid nitrogen. According to the requirements of ASTM E1681-03 code [3], evaluation of a crack growth caused by hydrogen was conducted perpendicular to the pre-crack at 25% B, 50% B and 75% B locations, where B is the specimen thickness. The results of a target and measured crack size (a_o), applied displacement (V_m), values of target and applied stress intensity factor (K_{IA}) as well as minimum threshold stress intensity factor ($K_{IH,min}$) are presented for representative specimens in [10]. According to the evaluation of the specimens, no subcritical crack growth of more than 0.25 mm average on three locations was identified for a minimum of three specimens tested per a position. The table in Appendix A presents in details the measurements of the crack size and fracture toughness values for L485ME steel grade, for specimens thickness 19 mm, width 38 mm, high 18.5 mm. TL orientated specimens were taken from BM (12 specimens), WM (9), HAZ (9), from SAWH pipes with the wall thickness of 22.2 mm.
i. Post-test macroscopic evaluation of specimens as well as evaluation with Scanning Electron Microscope (SEM) are presented in the next subchapter.

3.3. Macroscopic and microscopic analysis

All the prepared samples were analysed macroscopically and using electron microscopy. Macroscopic examination of the sample was performed with the use of Nikon SMZ 1500 stereo-microscope. Observations with a higher magnification microscope were performed with JEOL IT-800 HL Scanning Electron Microscope under 20 kV accelerating voltage, coupled with EDAX Octane Elect Plus system with the usage of TEAM software. The results of selected macroscopic examinations are presented in Figs. 2(a)-(c), whereas representative electron micrographs are shown in Figs. 3(a)-(c). Similar results were observed in the remaining samples, as listed in Appendix A. Therefore, no HIC was detected in 36 examined samples.

4. Governing equations

To estimate the fracture toughness, information about the flow conditions of the hydrogen-blended natural gas and the hydrogen content in the steel is required. Wang [26] derived the following empirical correlation, from experimental data, for the conditional fracture toughness K_{IQ} as a function of hydrogen content:

$$K_{IQ,d} = 58.31 - 19.84 \log c_H. \quad (1)$$

This relationship is based on dynamic charging $K_{IQ,d}$ at slow strain rate tension for API X70 pipe steel with a steel composition shown in Table 1.

Table 1. Chemical composition of X70 steel grade used in [26].

Tablica 1. Skład chemiczny stali gatunku X70 wykorzystanej w [26].

C	Mn	Si	P	S	Cu	Nb	Mo	Ti	Fe
0.041	1.76	0.281	0.016	0.006	0.193	0.067	0.194	0.023	balance

As it can be seen from Eq. (1), to estimate the fracture toughness, the hydrogen content c_H needs to be determined. This can be achieved by applying Sievert's law, which can be expressed in the following manner [12, 17]:

(a) (b) (c)

Fig. 2. Macrographs of fracture surfaces of (a) BM, (b) WM and (c) HAZ [10]

Rys. 2. Makrografia powierzchni pęknięcia dla (a) materiału bazowego, (b) materiału spoiny oraz (c) strefy wpływu ciepła [10]

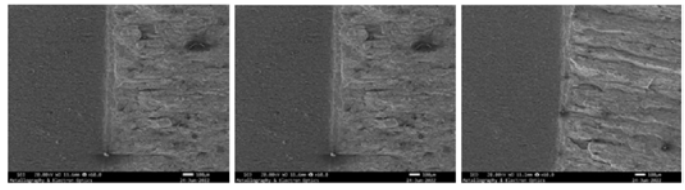

(a) (b) (c)

Fig. 3. Electron micrographs (SEM) showing the interface between the fatigue and the crack initiation zone of the fracture surface at (a) 25%, (b) 50% and (c) 75% of the J128B-BM4 specimen width [10]

Rys. 3. Mikrografia elektronowa (SEM), obrazująca styk pomiędzy zmęczeniem oraz strefą początku pęknięcia, dla powierzchni przełomu (a) 25%, (b) 50% oraz (c) 75% szerokości próbki oznaczonej jako J128B-BM4 [10]

$$c_H = k_0' \left(\frac{N_T}{N_L} + \frac{N_T}{N_L \exp(-E_b/RT)} + 1 \right) \sqrt{f} \exp\left(-\frac{\Delta H_s - \sigma_H V_H}{RT} \right), \quad (2)$$

with constant pre-factor k'_0, density of the lattice N_L, density of trap sites N_T, trap binding energy E_b, fugacity f, enthalpy change ΔH_s, hydrostatic stress σ_H and partial molar volume of hydrogen in solid solution V_H. The fugacity of hydrogen in the natural gas mixture is calculated from GERG-2008 [18]. The hydrostatic stress for thin-wall pipelines is obtained from

$$\sigma_H = \frac{pr_i}{2t_w}, \qquad d/t_w > 20, \quad (3)$$

with internal radius r_i, diameter d and wall thickness t_w. From Eq. (2), it can be seen that the pressure and temperature are necessary to calculate the hydrogen content.

From the laws of conservation of mass, momentum and energy, the one-dimensional transient gas flow can be expressed as follows [25]

$$\frac{\partial p}{\partial t} = \frac{a_s^2}{c_p T}\left(1 + \frac{T}{z}\left(\frac{\partial z}{\partial T}\right)_p\right)\left(\frac{q}{A} + \frac{\dot{m} z R T}{pA^2} w\right) - \left[\frac{\dot{m} z R T}{pA} - \frac{a_s^2 \dot{m}}{pA}\left(1 - \frac{p}{z}\left(\frac{\partial z}{\partial p}\right)_T\right)\right]\frac{\partial p}{\partial x} - \frac{a_s^2 \dot{m}}{TA}\left(1 + \frac{T}{z}\left(\frac{\partial z}{\partial T}\right)_p\right)\frac{\partial T}{\partial x} - \frac{a_s^2}{A}\frac{\partial \dot{m}}{\partial x}, \quad (4)$$

$$\frac{\partial T}{\partial t} = \frac{a_s^2}{c_p p}\left(1 - \frac{p}{z}\left(\frac{\partial z}{\partial p}\right)_T\right)\left(\frac{q}{A} + w\frac{\dot{m} z R T}{pA^2}\right) - \frac{\dot{m} z R T}{pA}\frac{\partial T}{\partial x} - \frac{a_s^2}{c_p}\left(1 + \frac{T}{z}\left(\frac{\partial z}{\partial T}\right)_p\right) \times \left[\frac{\dot{m} z R}{pA}\left(1 + \frac{T}{z}\left(\frac{\partial z}{\partial T}\right)_p\right)\frac{\partial T}{\partial x} - \frac{\dot{m} T R z}{p^2 A}\left(1 - \frac{p}{z}\left(\frac{\partial z}{\partial p}\right)_T\right)\frac{\partial p}{\partial x} + \frac{z T R}{pA}\frac{\partial \dot{m}}{\partial x}\right], \quad (5)$$

$$\frac{\partial \dot{m}}{\partial t} = -\frac{\dot{m}}{T}\left(1 + \frac{T}{z}\left(\frac{\partial z}{\partial T}\right)_p\right)\frac{\partial T}{\partial t} + \frac{\dot{m}}{p}\left(1 - \frac{p}{z}\left(\frac{\partial z}{\partial p}\right)_T\right)\frac{\partial p}{\partial t} - \frac{\dot{m}^2 z R}{pA}\left(1 + \frac{T}{z}\left(\frac{\partial z}{\partial T}\right)_p\right)\frac{\partial T}{\partial x} + \left(\frac{\dot{m}^2 T R z}{p^2 A}\left(1 - \frac{p}{z}\left(\frac{\partial z}{\partial p}\right)_T\right) - A\right)\frac{\partial p}{\partial x} - \frac{\dot{m} z T R}{pA}\frac{\partial \dot{m}}{\partial x} - w - \frac{pAg\sin(\theta)}{zTR}, \quad (6)$$

with time t, Cartesian coordinate x, pressure p, mass flow rate $\dot{m}$, temperature T, cross-sectional area A, frictional force w, friction factor f_r, gravitational acceleration g, angle of inclination θ, rate of heat transfer Ω, specific gas constant R, compressibility factor z, specific heat at constant pressure c_p, and isentropic wave speed a_s. The frictional force w per unit length is defined as

$$w = \frac{1}{8} f_r \rho v |v| \pi d_i, \quad (7)$$

with velocity v and internal diameter d_i. The friction factor is calculated from [24]

$$f_r = -0.8685 \ln\left(\frac{1.964 \ln(Re) - 3.8215}{Re} + \frac{\varepsilon}{3.71 d_i} \right)^{-2}, \quad (8)$$

where ε denotes the roughness and Re is the Reynolds number. The steady heat transfer between the fluid and the soil per unit length and the time is defined as

$$\Omega = -\pi d U (T - T_s), \quad (9)$$

where U is the total heat transfer coefficient and consists of the heat transfer between the gas and the inner wall, heat transfer through the pipe wall, and heat transfer between the outer wall and soil with temperature T_s. The thermodynamic properties are calculated from GERG-2008.

A semi-discretization approach is used for the numerical approximation. The spatial discretization is carried out using a classical three-point, second-order finite-difference scheme and the trapezoidal rule with a second-order backward difference formula [7] is used for the time-stepping.

5. Case study

In this section, simulations are conducted for a 177 km long X70M steel grade pipeline with an internal diameter of 1379.6 mm. The internal roughness of the pipeline 1.96 µm and the thickness of the pipe wall is 19.22 mm. The thermal conductivity of the steel is 45.3 Wm^{-1} K^{-1}. The soil temperature is 12 °C and its thermal conductivity is 2.0 Wm^{-1} K^{-1}. The depth of the pipeline cover is 1.5 m. The boundary conditions are set as follows: $\dot{m}(L,t)=\phi(t)$ (see Fig. 4), p(0,t) = 8.4 MPa and T(0,t) = 290.15 K. The natural gas has the following mol % composition: 96.803 CH_4, 1.773 C_2H_6, 0.395 C_3H_8, 0.063 i-C_4H_{10}, 0.057 n-C_4H_{10}, 0.010 i-C5H12, 0.007 n-C_5H_{12}, 0.009 C_6, 0.115 CO_2, and 0.768 N_2. The natural is blended at the entry with volume percentages of 10 % and 30 %. For the hydrogen solubility calculations, the following parameters are used [22, 23]: $E_{b,BM}$ = 36 kJ mol−1, $E_{b,HAZ}$ = 41 kJ mol^{-1}, $N_T = 2.3 \times 10^{19}$ sites cm^{-3}, k'_0 = 33 wppm $bar^{-0.5}$, $V_h = 2 \times 10^3$ mm^3 mol^{-1}, ΔH_s = 27 kJ mol^{-1}, $N_L = 5.2 \times 10^{23}$ sites cm^{-3}.

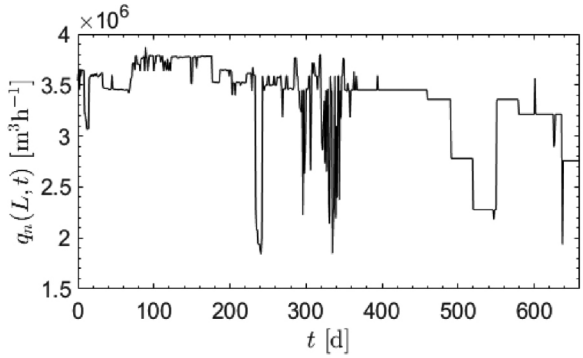

Fig. 4. Boundary condition ϕ(t) at the outlet of the pipeline
Rys. 4. Warunki brzegowe ϕ(t) na wyjściu z rurociągu

The simulation results for the hydrogen concentration and fracture toughness are presented in Fig. 5. Since the highest hydrogen concentration and the lowest fracture toughness are observed at the end of the pipeline section, the results are depicted for x ∈[100,150]. The highest hydrogen content and, as a consequence, the lowest fracture toughness, is recorded for HAZ because it contains bainite and martensite (see Table 2). The transformation into martensite causes an increase in the number of trapping sites and, as a result, the hydrogen content is higher. In [26] a critical hydrogen content of 1 wppm was found for the X70 pipeline steel. At this level the fracture toughness shows a significant reduction. As it can be observed from Table 2, the hydrogen concentration for HAZ with 30 % and 50 % vol. H_2, exceeds this threshold value.

Table 2. Calculated values of the highest hydrogen content and the lowest fracture toughness
Tablica 2. Obliczone wartości najwyższej zawartości wodoru oraz najniższej odporności na pękanie

Microstructure	H_2 in natural gas [vol. %]	c_H [wppm]	$K_{IQ,d}$ [MPa $m^{0.5}$]
BM	30	0.38	78.3
BM	50	0.48	73.4
HAZ	30	2.90	37.2
HAZ	50	3.73	32.2

The average $K_{IH,min}$ for BM and HAZ is 72.2 and 68.8 MPa $m^{0.5}$, respectively (see Appendix A). In line with [5], $K_{IH,min}$ is equal to 50% of the applied K_{IA}. Considering that K_{IA} values exceed 110 MPa $m^{0.5}$ for all specimens, the threshold stress intensity factor K_{IH} value of 55 MPa $m^{0.5}$ can also be qualified as a minimum for all specimens. The latter value is used to evaluate the fracture toughness of L485ME steel that is exposed to hydrogen. This infers that only HAZ is vulnerable to HE and that blending 30 % and 50 % vol. H_2 in the natural gas for BM material may not cause fracture toughness problems for L485ME steel grade. It should be noted that the results are valid within the assumptions and approximations made in the simulations. The validity of a comparison of threshold stress intensity factor K_{IH} [3] with conditional calculated values of $K_{IQ,d}$ [26] is ensured by requirements of the specimen size [3, 6] meeting the criteria for plane strain conditions.

The simulations are repeated for HAZ with 50 % vol. H_2 in the natural gas and the following material parameters: E_b = 30 kJ mol^{-1}, $N_T = 10 \times 10^{-7}$ mol mm^{-3}, and $N_L = 8.5 \times 10^{-4}$ mol mm^{-3}. These parameters are considered as a rough estimation for pressurized specimens, pipes, and pressure vessels produced of ferritic and martensitic steels [11]. The remaining parameters required to calculate the hydrogen concentration are kept the same. The results are depicted in Fig. 6 and significantly differ from the results in Table 2. The hydrogen content varies between 0.093 and 0.105 wppm and fracture toughness between 103.08 and 105.52 MPa $m^{0.5}$. However, simulations showed that the results are sensitive to the binding energy, which highly depends on the material imperfections, the interatomic forces at the defect sites, and the dilation of the crystal lattice close to the crystal defects [11].

In [26], a critical hydrogen content of 1 wppm for the X70 pipeline steel was found. Above this threshold the fracture toughness significantly decreased. The results in Table 2 show that the hydrogen content of HAZ exceeds this critical concentration. From the experimental results reported in the Appendix, a mean $K_{IH,min}$ of 72.2 and 68.8 MPa $m^{0.5}$ was found for BM and HAZ, respectively. In line with [5], $K_{IH,min}$ is equal to 50% of the applied K_{IA}. For all specimens, K_{IA} values exceed 110 MPa $m^{0.5}$, therefore the threshold stress intensity factor KIH of 55 MPa $m^{0.5}$ can also be considered as a minimum. The latter value is used to evaluate the fracture toughness of L485ME steel

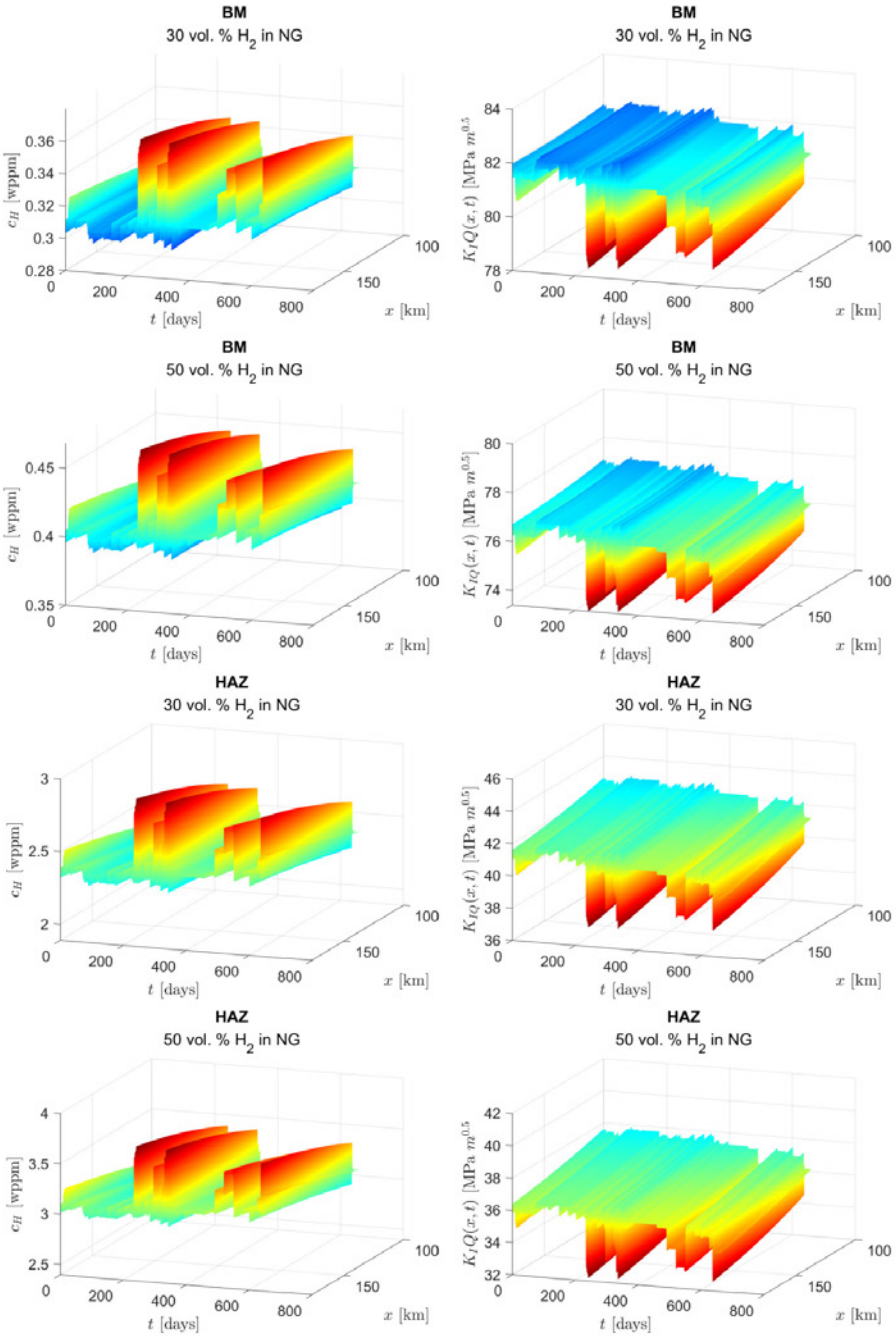

Fig. 5. Hydrogen content and fracture toughness for BM and HAZ with 30 % and 50 % vol. H_2 in natural gas

Rys. 5. Zawartość wodoru oraz odporność na pękanie dla materiału bazowego oraz strefy wpływu ciepła, dla zawartości H_2 w gazie ziemnym 30 % oraz 50 % objętościowo

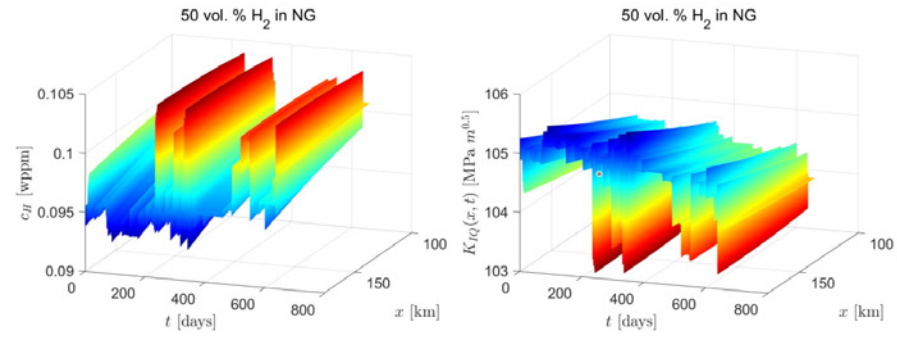

Fig. 6. Hydrogen content and fracture toughness for HAZ and 50 % vol. H_2 in natural gas using the parameters in [11]

Rys. 6. Zawartość wodoru oraz odporność na pękanie dla strefy wpływu ciepła i 50 % objętościowej zawartości H_2 w gazie ziemnym z wykorzystaniem parametrów wg [11]

Appendix A. Experimental data of the target and measured crack size, applied displacement, target and an applied stress intensity factor as well as minimum threshold stress intensity factor for L485ME steel grade 22.2 wall thickness pipes [10].

Załącznik A. Dane doświadczalne docelowego oraz zmierzonego wymiaru pęknięcia, zastosowane wydłużenie, docelowy oraz zastosowany współczynnik intensywności naprężeń, jak również minimalny graniczny współczynnik intensywności naprężeń dla rur o grubości ścianki 22.2 ze stali L485ME [10].

		Wall	a_0	V_m	K_{IA}	a_0	K_{IA}	$K_{IH,min}$
		thickness	target	applied	target	measured	applied	minimum
No.	Specimen ID	[mm]	[mm]	[mm]	[MPa m$^{0.5}$]	[mm]	[MPa m$^{0.5}$]	[MPa m$^{0.5}$]
1	J128A-BM1	22.2	24.97	0.907	125	22.431	147.6	73.8
2	J128A-BM2	22.2	24.86	0.864	125	22.643	139.6	69.8
3	J128A-BM3	22.2	25.18	0.913	125	22.945	145.9	72.9
4	J128A-BM4	22.2	24.81	0.930	125	21.853	154.8	77.4
5	J128B-BM1	22.2	24.77	0.814	125	20.465	143.5	71.8
6	J128B-BM2	22.2	24.82	0.946	125	22.771	152.0	76.0
7	J128B-BM3	22.2	24.49	0.863	125	20.845	149.7	74.8
8	J128B-BM4	22.2	24.76	0.866	125	22.407	141.1	70.5
9	J128C-BM1	22.2	25.33	0.760	125	19.340	140.8	70.4
10	J128C-BM2	22.2	25.33	0.844	125	22.617	136.4	68.2
11	J128C-BM3	22.2	25.18	0.874	125	22.660	141.0	70.5
12	J128C-BM4	22.2	25.24	0.920	125	24.080	141.0	70.5
13	J128A-W1	22.2	24.83	0.728	125	20.714	127.0	63.5
14	J128A-W3	22.2	25.07	0.854	125	22.928	136.5	68.2
15	J128A-W4	22.2	24.95	0.638	125	20.317	113.2	56.6
16	J128A-HAZ1	22.2	25.29	0.945	125	23.056	150.2	75.1
17	J128A-HAZ2	22.2	24.83	0.641	125	19.732	116.7	58.4
18	J128A-HAZ3	22.2	24.61	0.816	125	22.350	133.2	66.6
19	J128B-W1	22.2	24.47	0.847	125	21.527	142.8	71.4
20	J128B-W2	22.2	24.53	0.863	125	21.932	143.2	71.6
21	J128B-W3	22.2	24.55	0.719	125	21.330	122.3	61.1
22	J128B-HAZ2	22.2	24.64	0.889	125	21.266	151.6	75.8
23	J128B-HAZ3	22.2	24.12	0.750	125	20.176	133.9	66.9
24	J128B-HAZ4	22.2	24.59	0.814	125	21.626	136.8	68.4
25	J128C-W1	22.2	24.81	0.867	125	21.154	148.5	74.3
26	J128C-W2	22.2	24.97	0.871	125	22.082	143.7	71.9
27	J128C-W4	22.2	25.17	0.745	125	22.707	120.5	60.2
28	J128C-HAZ1	22.2	25.29	0.890	125	23.925	137.2	68.6
29	J128C-HAZ4	22.2	25.24	0.879	125	23.184	139.2	69.6
30	J128C-HAZ5	22.2	25.12	0.876	125	23.067	139.2	69.6

grade that is exposed to hydrogen. The simulation results indicate that only the HAZ material seems to be sensitive to hydrogen environmental cracking. This would imply that the injection of 30 % and 50 % vol. H_2 in the natural gas for the BM material and parameters used for L485ME steel grade may not cause fracture toughness problems. By all means, the results are valid within the assumptions and approximations considered in the case study.

6. Conclusions

In this work, the vulnerability of L485ME low-alloy steel grade (API notation X70M) to hydrogen embrittlement was investigated. A hydraulic model was used to estimate the pipeline operating conditions and as a result the hydrogen concentration and fracture toughness. The simulations were carried out under the assumption that thermodynamic equilibrium exists between the steel and hydrogen. The calculations for a real pipeline while using the material parameters for X70M showed that the fracture toughness parameter for HAZ drastically decreases for 30 % and 50 % vol. H_2 in natural gas. On the other hand, considering the rough estimated material parameters proposed in the literature for ferritic and martensitic steels, the results indicate that for HAZ and 50 % of H_2 the fracture toughness is significantly higher. Nevertheless, the methodology presented in this work can be applied when examining the susceptibility of steel pipelines to hydrogen-induced embrittlement.

Acknowledgements

The authors wish to thank Corinth Pipeworks S.A. for facilitating the experimental data and Reviewers for their valuable comments and suggestions.

Declaration of interest

Conflict of Interest: The authors declare that there are no conflicts of interest that are directly or indirectly related to the research.

Funding: The authors declare that the research has not received any funding.

Compliance with Ethical Standards: The research has not involved tests on either humans or animals.
Availability of data and material: All data generated or analysed during this study are available on request.
Code availability: The published article includes all information about the software and algorithms used during this study.
Al declaration: During the preparation of this work the authors didn't used any AI tools as part of the research process.

Authorship contributions

Ferdinand Uilhoorn and Maciej Witek: Conceptualization, Methodology, Model.
Ferdinand Uilhoorn and Maciej Witek: Data curation, Writing – Original draft preparation.
Ferdinand Uilhoorn and Maciej Witek: Visualization, Investigation.
Ferdinand Uilhoorn and Maciej Witek: Software, Validation.
Ferdinand Uilhoorn and Maciej Witek: Writing – Reviewing and Editing.

LITERATURA

[1] API Spec 5L, 46th edition, April 2018, Line pipe, Washington. Technical report.
[2] EN-ISO 3183:2019. 2019. "Petroleum and natural gas industries – Steel pipe for pipeline transportation system". Technical report, Technical Comittee: ISO/TC 67/SC 2.
[3] ASTM E1681-03. 2020. "Standard Test Method for Determining Threshold Stress Intensity Factor for Environment Assisted Cracking of Metallic Materials". ASTM International. Technical report.
[4] ASME B31.12:2019. 2020. "Hydrogen piping and pipelines, ASME code for pressure piping". Technical report, The American Society of Mechanical Engineer.
[5] ASME BPVC Section VIII, Division 3. 2021. "Alternative Rules for Construction of High Pressure Vessels, ASME Boiler and Pressure Vessel Code". Technical report, The American Society of Mechanical Engineer.
[6] ASTM E399-22. 2022. "Standard Test Method for Linear-Elastic Plane-Strain Fracture Toughness KIC of Metallic Materials." ASTM International. Technical report.
[7] Bank Randolph E., Coughran Jr. William M., Wolfgang Fichtner, Eric Grosse, Donald J.Rose, and Kent Smith. 1985. "Transient simulation of silicon devices and circuits". IEEE Trans. Electron Devices, 32(10):1992–2007.
[8] Bhardwaj Utkarsh, Ângelo Manuel Palos Teixeira, and Carlos Guedes Soares. 2021. "Burst strength assessment of X100 to X120 ultra-high strength corroded pipes". Ocean Eng., 241:110004.
[9] Giovambattista Bilotta, Gilbert Henaff, Damien Halm, and Mandana Arzaghi. 2017. "Experimental measurement of out-of-plane displacement in crack propagation under gaseous hydrogen". Int. J. Hydrogen Energy, 42(15):10568–10578.
[10] Corinth Pipeworks S.A. 2022. "Hydrogen KIH qualification test report KIH testing of 40" x 22.2 mm /L485ME SAWH". non-published.

[11] Drexler Andreas, Tom Depover, Silvia Leitner, Kim Verbeken, and Werner Ecker. 2020. "Microstructural based hydrogen diffusion and trapping models applied to Fe–CX alloys". J. Alloys Compd., 826:154057.
[12] Drexler Andreas, Florian Konert, Oded Sobol, Michael Rhode, Josef Domitner, Christof Sommitsch, and Thomas Böllinghaus. 2022. "Enhanced gaseous hydrogen solubility in ferritic and martensitic steels at low temperatures". Int. J. Hydrogen Energy, 47(93):39639–39653.
[13] Goutam Ghosh, Paul Rostron, Rajnish Garg, and Ashoutosh Panday. 2018. "Hydrogen induced cracking of pipeline and pressure vessel steels: A review". Eng. Fract. Mech., 199:609–618.
[14] Xiaofei Guo, Tianyi Li, Zhendong Sheng, Martin Christ, Rahul Sharma, Marcus Söker, Uwe Reisgen, and Wolfgang Bleck. 2022. "Impact of welding simulated heat treatment on hydrogen embrittlement behavior of high-strength fine-grained steels". Eng. Fail. Anal., 140:106602.
[15] Hagen Anette Brocks and Antonio Alvaro. 2020. "Hydrogen Influence on Mechanical Properties in Pipeline Steel – state of the art". SINTEF Rapp.
[16] Minoru Ichimura, Yasushi Sasajima, and Mamoru Imabayashi. 1991. "Grain boundary effect on diffusion of hydrogen in pure aluminum". Mater. Trans. JIM, 32(12): 1109–1114.
[17] Kirchheim Reiner. 1982. "Solubility, diffusivity and trapping of hydrogen in dilute alloys. deformed and amorphous metals—II". Acta Metall., 30(6):1069–1078.
[18] Kunz Oliver, Wolfgang Wagner. 2012. "The GERG-2008 Wide-Range equation of state for natural gases and other mixtures: An expansion of GERG-2004". J. Chem. Eng. Data, 57(11):3032–3091.
[19] Latifi Amin, Reza Miresmaeili, and Amir Abdollah-Zadeh. 2017. "The mutual effects of hydrogen and microstructure on hardness and impact energy of SMA welds in X65 steel". Materials Science and Engineering: A, 679:87–94.
[20] Mohammadijoo Mohse, Jonas Valloton, Laurie Collins, Hani Henein, and D. G. Ivey 2018. "Characterization of martensite-austenite constituents and micro-hardness in intercritical reheated and coarse-grained heat affected zones of API X70 HSLA steel". Mater. Charact., 142:321–331.
[21] Ohaeri Enyinnaya, Joseph Omale, Rahman K. M. Mostafijur, and Jerzy Szpunar. 2020. "Effect of post-processing annealing treatments on microstructure development and hydrogen embrittlement in API 5L X70 pipeline steel". Mater. Charact., 161:110124.
[22] Olden Vigdis, Antonio Alvaro, and Odd M. Akselsen 2012. "Hydrogen diffusion and hydrogen influenced critical stress intensity in an API X70 pipeline steel welded joint – experiments and FE simulations". International Journal of Hydrogen Energy, 37(15):11474–11486.
[23] Skjellerudsveen Magnus, Odd M. Akselsen, Olden Vigdis, Johnsen Roy, and Anna Smirnova. 2010. "Effect of microstructure and temperature on hydrogen diffusion in X70 grade pipeline steel and its weldments".
[24] Techo Robert, R. R. Tickner, and R. E. James. 1965. "An Accurate Equation for the Computation of the Friction Factor for Smooth Pipes From the Reynolds Number". J. Appl. Mech., 32(2):443–443.
[25] Uilhoorn Ferdinand. 2017. "Comparison of Bayesian estimation methods for modeling flow transients in gas pipelines". Journal of Natural Gas Science and Engineering, 38: 159–170.
[26] Wang Rong. 2009. "Effects of hydrogen on the fracture toughness of a X70 pipeline steel". Corros. Sci., 51(12):2803–2810.
[27] Wasim Muhammad, Milos B. Djukic, and Tuan Duc Ngo. 2021. "Influence of hydrogen-enhanced plasticity and decohesion mechanisms of hydrogen embrittlement on the fracture resistance of steel". Eng. Fail. Anal., 123:105312.
[28] Witek Maciej. 2015. "Possibilities of using X80, X100, X120 high-strength steels for onshore gas transmission pipelines". Journal of Natural Gas Science and Engineering, 27:374–384.
[29] Yazdipour Nima, Druce Dunne, and Elena V. Pereloma. 2012. "Effect of grain size on the hydrogen diffusion process in steel using cellular automaton approach". Mater. Sci. Forum, 706-709:1568–1573.
[30] Yazdipour Nima, Haq J. Ayesha, Khairul Muzaka, and Elena V. Pereloma. 2012. "2D modelling of the effect of grain size on hydrogen diffusion in X70 steel". Comput. Mater. Sci., 56:49–57.

Prof. dr hab. inż. Jan Pawełek doktorem honoris causa Uniwersytetu Przyrodniczego w Lublinie

W dniu 16 listopada 2023 roku odbyła się uroczystość uhonorowania prof. dr hab. inż. Jana Pawełka tytułem doktora honoris causa Uniwersytetu Przyrodniczego w Lublinie. Ta najwyższa godność akademicka jaką może nadać uczelnia wyższa, jest wyrazem uznania wkładu naukowego Profesora – wybitnego naukowca, innowatora i lidera w dziedzinie inżynierii i ochrony środowiska.

Osiągnięcia naukowe profesora Jana Pawełka obejmują tematykę: programowania, projektowania, budowy i użytkowania systemów zaopatrzenia w wodę i odprowadzania ścieków na obszarach wiejskich; hydrotransportu granulowanego węgla aktywnego stosowanego w oczyszczaniu wody i ścieków; zużycia wody w gospodarstwach wiejskich, a także jakości wody powierzchniowej i technologii jej oczyszczania w powiązaniu z możliwością stosowania rezerwy zbiornikowej.

Profesor Jan Pawełek jest autorem i współautorem ponad 200 prac, w tym 115 oryginalnych prac twórczych, 38 publikacji popularnonaukowych, podręcznika, 63 prac niepublikowanych: ekspertyzy, projekty i sprawozdania, a także redaktorem prac zbiorowych i monografii.

Profesor Jan Pawełek był promotorem 4 rozpraw doktorskich oraz recenzentem: 19 prac doktorskich, 14 prac habilitacyjnych, 4 dorobków na stanowisko prof. nadzwyczajnego i 1 na stanowisko prof. zwyczajnego, 13 wniosków o tytuł naukowy profesora, 4 wniosków o uzyskanie przez jednostki naukowe uprawnień do nadawania stopni naukowych. Był także przewodniczącym i członkiem 52 komisji habilitacyjnych.

W swojej karierze zawodowej Profesor Jan Pawełek był prodziekanem oraz dziekanem Wydziału Inżynierii Środowiska i Geodezji Uniwersytetu Rolniczego w Krakowie, kierownikiem Katedry Inżynierii Sanitarnej i Gospodarki Wodnej, członkiem i przewodniczącym wielu komisji rektorskich, senackich i wydziałowych oraz członkiem Centralnej Komisji ds. Stopni i Tytułów. Z wielkim oddaniem udzielał się także na rzecz środowiska inżynierskiego, szczególnie w Polskim Zrzeszeniu Inżynierów i Techników Sanitarnych, w którym pełnił i nadal pełni zaszczytne funkcje. Był m.in. wiceprezesem oraz prezesem Zarządu Oddziału w Krakowie, członkiem Zarządu Głównego, a w obecnej kadencji jest jego wiceprezesem. Działał także w Radzie FSN-T NOT oraz Krakowskim Towarzystwie Technicznym.